



The principles of Tomography

following the book

A. C. Kak, M. Slaney,
Principles of Computerized Tomographic Imaging,
IEEE Press, New York, 1988

presented by
B. Schillinger

Heinz Maier-Leibnitz Institut (FRM II)
Technische Universität München

Germany



- 1. Introduction**
- 2. The tomography principle**
 - 2.1 Projection and Radon Transform*
 - 2.2. The Fourier Slice Theorem*
 - 2.3 Filtered Backprojection*
 - 2.4 Number of projections*
- 3. Beam geometries for tomography**
- 4. The neutron case - flight tube vs. beam guide**
- 7. Discussion**



1. Introduction

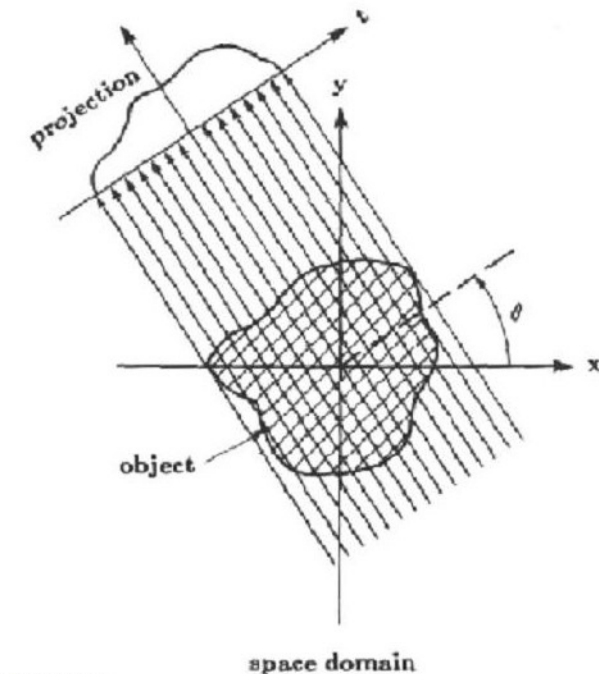
- A radiography is a shadow image of the investigated sample.
- Information about the internal distribution of the attenuation coefficient within the sample is lost in the projection.
- If the sample is rotated and many different views are taken, a tomographic reconstruction of that internal distribution can be performed.
- Mathematical models assume either a perfect parallel beam or a perfect point source.
- Neither case is given for neutron tomography.
- It is therefore of great importance to shape the beam as to approximate ideal beam geometry best as possible.

2. The tomography principle

2.1 Projection and Radon Transform

The following assumptions are made:

- the examined object is penetrated by a bundle of parallel rays.
The procedure can be described in a plane (x,y).
- The beam is attenuated by the two-dimensional attenuation coefficient $\mu(x,y)$.
- Scattered neutrons do not hit the detector, so scattering looks like absorption.
- The beam is monoenergetic.

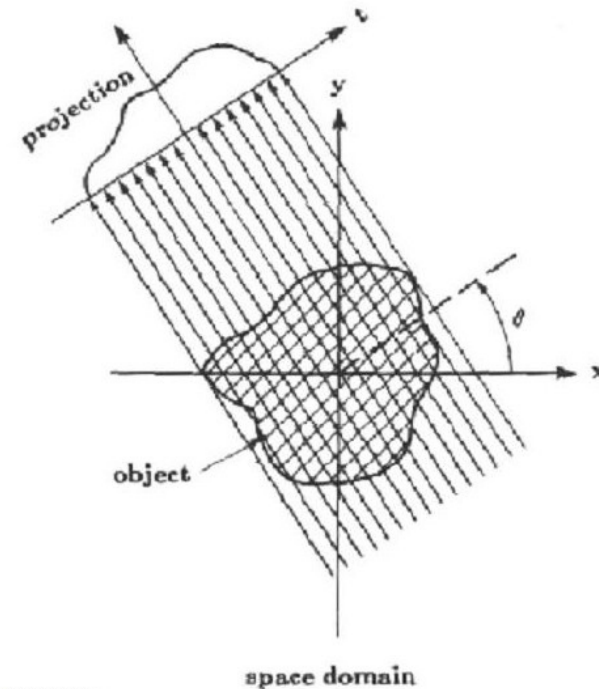


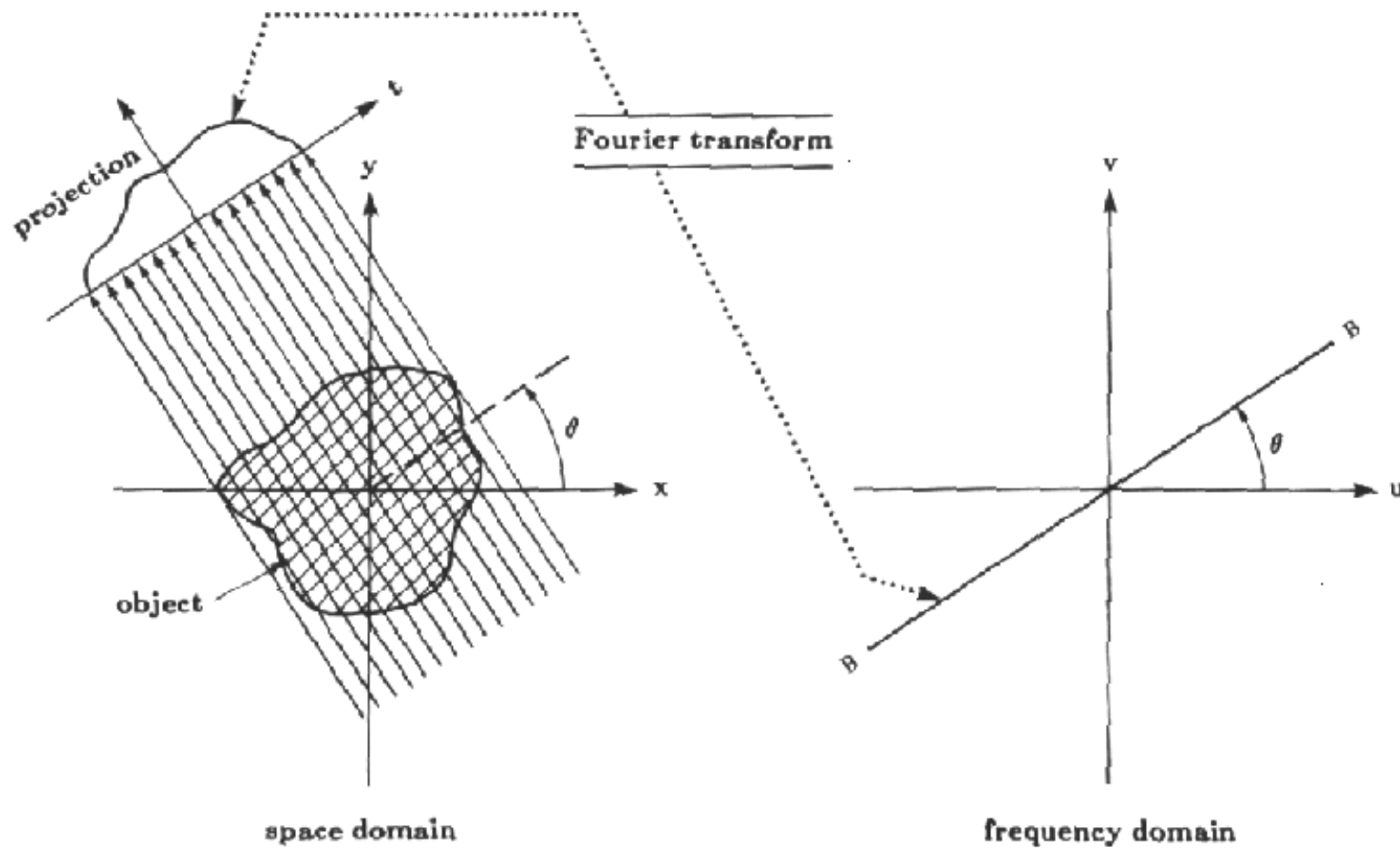
Each detector element is hit by a number of neutrons

$$N = N_0 \cdot e^{-\int_{\text{beam path}} \mu(x,y) ds}$$

with N_0 = number of incident neutrons
and the linear attenuation coefficient $\mu(x,y)$ at position (x,y) .

Integration is performed along the straight beam path s
through the plane.





Projection $P_{\theta}(t)$ of a two-dimensional slice
and the position of its fourier transform $P_{\theta}(\omega)$ in frequency domain.



We can give the projection of the two-dimensional slice as a one-dimensional function of the variable t perpendicular to the rays:

$$p_{\theta}(t) = \int_{ray(\theta,t)} \mu(x, y) ds$$

We can give the projection of the two-dimensional slice as a one-dimensional function of the variable t perpendicular to the rays:

$$p_{\theta}(t) = \int_{ray(\theta,t)} \mu(x, y) ds$$

$$= \int_{-\infty}^{+\infty} \int_{-\infty}^{+\infty} \delta(x \cos \theta + y \sin \theta - t) \mu(x, y) dx dy$$

with $t = x \cos \theta + y \sin \theta$

We can give the projection of the two-dimensional slice as a one-dimensional function of the variable t perpendicular to the rays:

$$p_{\theta}(t) = \int_{ray(\theta,t)} \mu(x, y) ds$$
$$= \int_{-\infty}^{+\infty} \int_{-\infty}^{+\infty} \delta(x \cos \theta + y \sin \theta - t) \mu(x, y) dx dy$$

$$\text{with } t = x \cos \theta + y \sin \theta$$

This is the *Radon Transform* .



It can be derived from measurement as

$$p_{\theta}(t) = -\ln \frac{N_{\theta}(t)}{N_0(t)}$$



It can be derived from measurement as

$$p_{\theta}(t) = -\ln \frac{N_{\theta}(t)}{N_0(t)}$$

For parallel beam geometry, an angular range of 0 to 180° it is sufficient.

It can be derived from measurement as

$$p_{\theta}(t) = -\ln \frac{N_{\theta}(t)}{N_0(t)}$$

For parallel beam geometry, an angular range of 0 to 180° it is sufficient.

The integration causes the loss of the spatial information about the distribution of $\mu(x,y)$ along the ray path.

It can be derived from measurement as

$$p_{\theta}(t) = -\ln \frac{N_{\theta}(t)}{N_0(t)}$$

For parallel beam geometry, an angular range of 0 to 180° it is sufficient.

The integration causes the loss of the spatial information about the distribution of $\mu(x,y)$ along the ray path.

But as each ray represents an independent measurement, the spatial information perpendicular to the ray direction (i.e. in direction θ,t) is still present.

The one-dimensional Fourier-Transform of the projection $P_\theta(\omega)$ is

$$P_\theta(\omega) = \int_{-\infty}^{+\infty} p_\theta(t) e^{-2\pi i \omega t} dt$$

2.2 *The Fourier Slice Theorem*

The one-dimensional Fourier-Transform of the projection $P_\theta(\omega)$ is

$$P_\theta(\omega) = \int_{-\infty}^{+\infty} p_\theta(t) e^{-2\pi i \omega t} dt$$

and the two-dimensional Fourier-Transform $S(u,v)$ of the slice to be reconstructed is:

$$S(u, v) = \int_{-\infty}^{+\infty} \int_{-\infty}^{+\infty} \mu(x, y) e^{-2\pi i (ux+vy)} dx dy$$



These combined deliver the Fourier Slice Theorem:

$$P_{\theta}(\omega) = \mathcal{S}(\omega \cos \theta, \omega \sin \theta) \equiv \mathcal{S}(\omega, \theta)$$

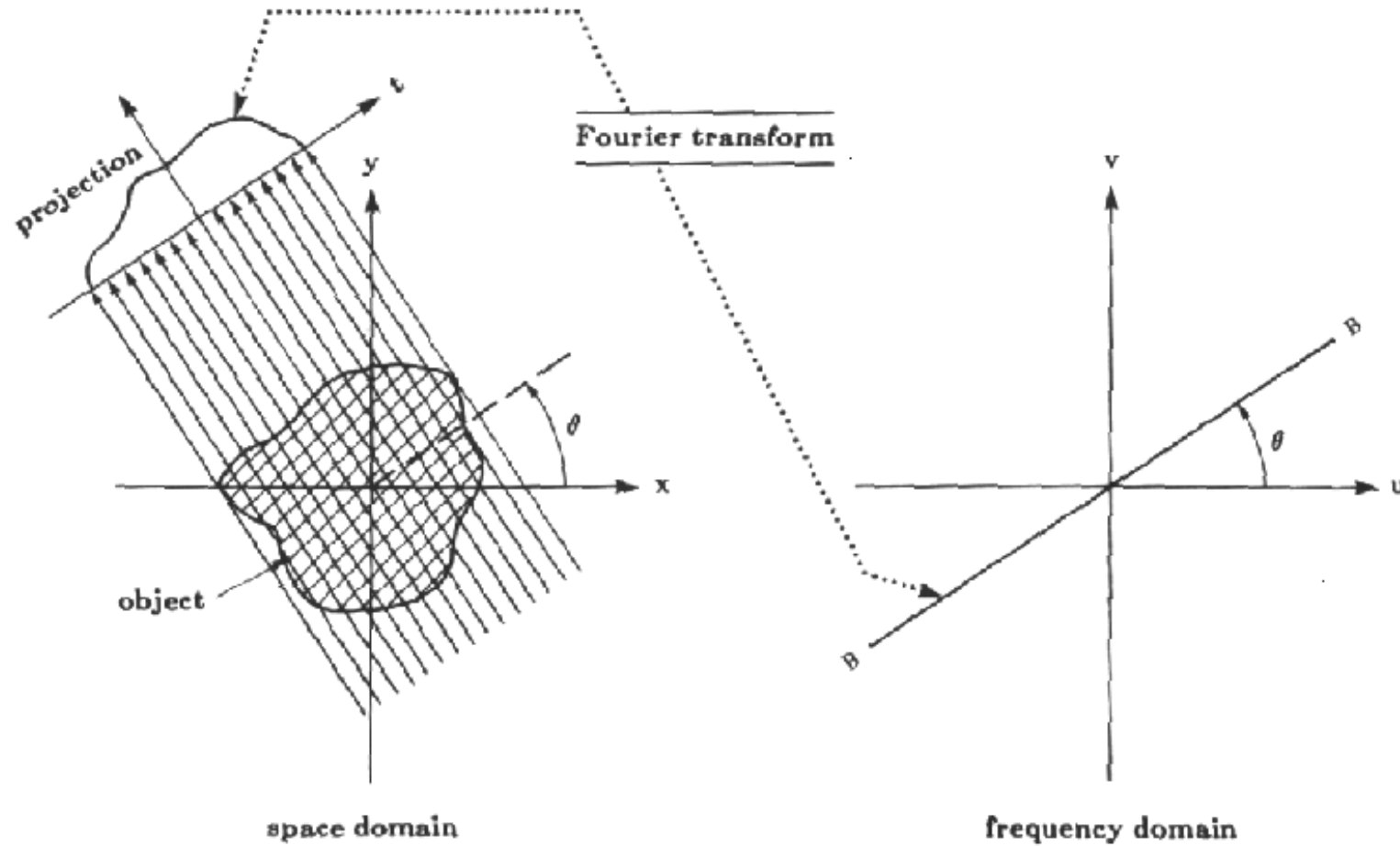
These combined deliver the Fourier Slice Theorem:

$$P_{\theta}(\omega) = \mathcal{S}(\omega \cos \theta, \omega \sin \theta) \equiv \mathcal{S}(\omega, \theta)$$

Which can be worded as:

“The one-dimensional Fourier Transform $P_{\theta}(\omega)$ of a parallel projection of a distribution $\mu(x,y)$, taken under an angle θ , is identical with a single line within the two-dimensional Fourier Transform $S(u,v)$ of the distribution $\mu(x,y)$ that encloses the angle θ with the u -axis.”

For reminder, again the representation in the spatial
and in the Fourier Domain:





In theory, it would be possible to fill the entire Fourier space by measuring an infinite number of projections and then to obtain the distribution $\mu(x,y)$ by a two-dimensional Fourier Backtransform of $S(u,v)$:

$$\mu(x, y) = \int_{-\infty}^{+\infty} \int_{-\infty}^{+\infty} S(u, v) e^{2\pi i(ux+vy)} du dv$$

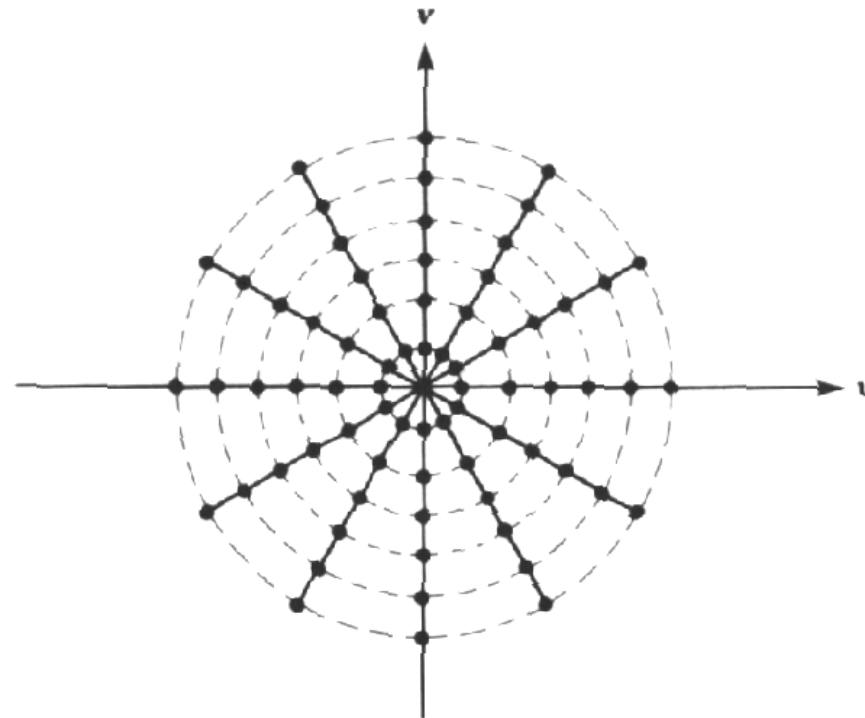


2.3 ***Filtered Backprojection***

In reality, the number of rays and the number of projections is limited.

2.3 Filtered Backprojection

In reality, the number of rays and the number of projections is limited.
The function $S(u,v)$ is known only at a few points on radial lines.



Measured values in frequency domain



These points must be interpolated to a quadratic mesh.



These points must be interpolated to a quadratic mesh.

With increasing radial distance, the density of measured values decreases, and interpolation uncertainty increases.



These points must be interpolated to a quadratic mesh.

With increasing radial distance, the density of measured values decreases, and interpolation uncertainty increases.

A simple reconstruction can be performed by simply summing up the two-dimensional Fourier Transforms of the single lines.



These points must be interpolated to a quadratic mesh.

With increasing radial distance, the density of measured values decreases, and interpolation uncertainty increases.

A simple reconstruction can be performed by simply summing up the two-dimensional Fourier Transforms of the single lines.

Because of the linearity of the Fourier Transform, this can be done either in spatial or in frequency domain.



These points must be interpolated to a quadratic mesh.

With increasing radial distance, the density of measured values decreases, and interpolation uncertainty increases.

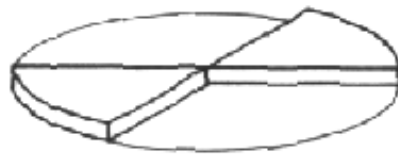
A simple reconstruction can be performed by simply summing up the two-dimensional Fourier Transforms of the single lines.

Because of the linearity of the Fourier Transform, this can be done either in spatial or in frequency domain.

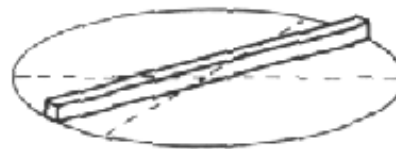
But as the density of measured values decreases towards high frequencies, the high frequencies do not get enough weight, and the reconstructed image appears smoothed or smeared.

Each of k projektions over 180° must deliver the information for a "cake slice" of width $2\pi|\omega|/k$.

But as it delivers only a single line, it is weighted with a ramp filter of height $2\pi|\omega|/k$, so that the new wedge has the same "mass" as the cake slice.



(a)



(b)



(c)

required, real and filtered representation
of the data in frequency domain



The filter $|\omega|$ can be obtained mathematically exact by transformation to polar coordinates in frequency space. Then we obtain

The filter $|\omega|$ can be obtained mathematically exact by transformation to polar coordinates in frequency space. Then we obtain

$$\begin{aligned}\mu(x, y) &= \int_0^{\pi} \int_0^{+\infty} S(\omega, \theta) e^{2\pi i \omega (x \cos \theta + y \sin \theta)} |\omega| d\omega d\theta \\ &= \int_0^{\pi} \int_0^{+\infty} S(\omega, \theta) e^{2\pi i \omega t} |\omega| d\omega d\theta \quad \text{with } t = x \cos \theta + y \sin \theta\end{aligned}$$

The filter $|\omega|$ can be obtained mathematically exact by transformation to polar coordinates in frequency space. Then we obtain

$$\begin{aligned}\mu(x, y) &= \int_0^{\pi} \int_0^{+\infty} S(\omega, \theta) e^{2\pi i \omega (x \cos \theta + y \sin \theta)} |\omega| d\omega d\theta \\ &= \int_0^{\pi} \int_0^{+\infty} S(\omega, \theta) e^{2\pi i \omega t} |\omega| d\omega d\theta \quad \text{with } t = x \cos \theta + y \sin \theta\end{aligned}$$

If we now substitute the one-dimensional Fourier Transform $P_{\theta}(\omega)$ of the projection at angle θ for the two-dimensional Fourier Transform $S(\omega, \theta)$, we obtain

$$\begin{aligned}\mu(x, y) &= \int_0^{\pi} \left[\int_0^{+\infty} P_{\theta}(\omega) e^{2\pi i \omega t} |\omega| d\omega \right] d\theta \quad \text{with } t = x \cos \theta + y \sin \theta \\ &= \int_0^{\pi} Q_{\theta}(x \cos \theta + y \sin \theta) d\theta \quad \text{with } Q_{\theta}(t) = \int_0^{+\infty} P_{\theta}(\omega) e^{2\pi i \omega t} |\omega| d\omega\end{aligned}$$

The filter $|\omega|$ can be obtained mathematically exact by transformation to polar coordinates in frequency space. Then we obtain

$$\begin{aligned}\mu(x, y) &= \int_0^{\pi} \int_0^{+\infty} S(\omega, \theta) e^{2\pi i \omega (x \cos \theta + y \sin \theta)} |\omega| d\omega d\theta \\ &= \int_0^{\pi} \int_0^{+\infty} S(\omega, \theta) e^{2\pi i \omega t} |\omega| d\omega d\theta \quad \text{with } t = x \cos \theta + y \sin \theta\end{aligned}$$

If we now substitute the one-dimensional Fourier Transform $P_{\theta}(\omega)$ of the projection at angle θ for the two-dimensional Fourier Transform $S(\omega, \theta)$, we obtain

$$\begin{aligned}\mu(x, y) &= \int_0^{\pi} \left[\int_0^{+\infty} P_{\theta}(\omega) e^{2\pi i \omega t} |\omega| d\omega \right] d\theta \quad \text{with } t = x \cos \theta + y \sin \theta \\ &= \int_0^{\pi} Q_{\theta}(x \cos \theta + y \sin \theta) d\theta \quad \text{with } Q_{\theta}(t) = \int_0^{+\infty} P_{\theta}(\omega) e^{2\pi i \omega t} |\omega| d\omega\end{aligned}$$

This Equation describes a filter operation with the filter $|\omega|$.

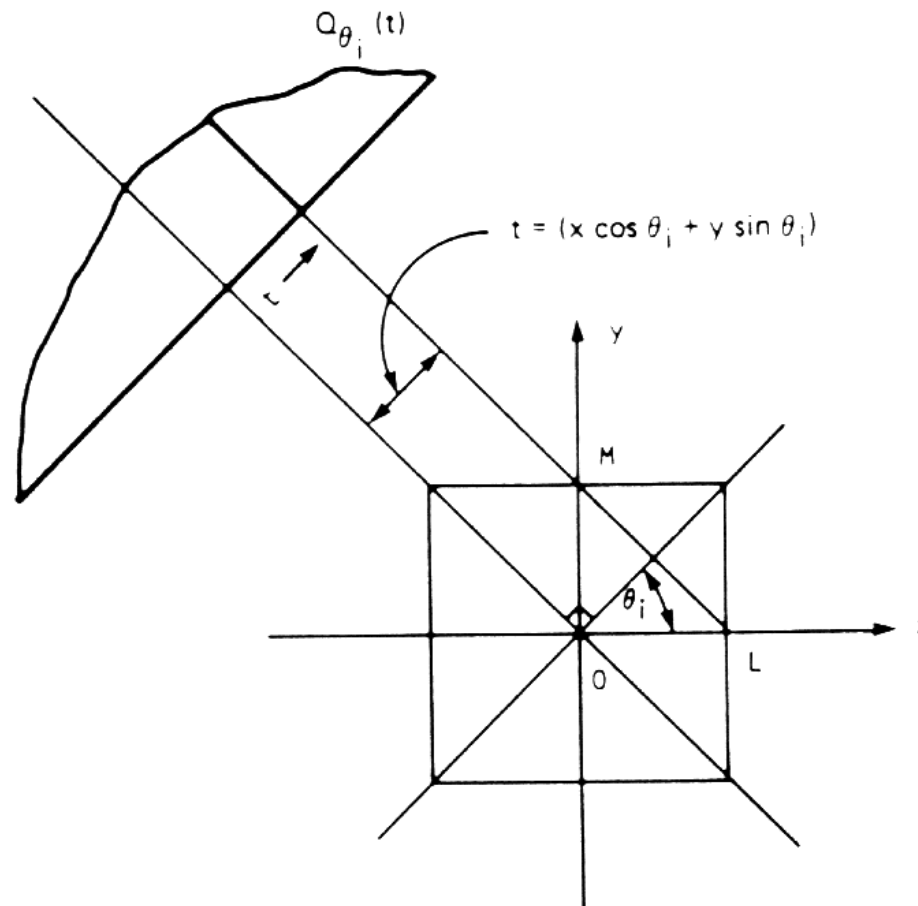


$Q_{\theta}(t)$ is called "filtered projection".

These filtered projections are "backprojected" onto the reconstruction field:
Each filtered projections $Q_{\theta}(t)$ contributes the same value to all points
of the reconstruction field along the original ray.

The filtered backprojection is being "smeared" along the original ray path
across the reconstruction field.

The filtered backprojection is being "smeared" along the original ray path across the reconstruction field.



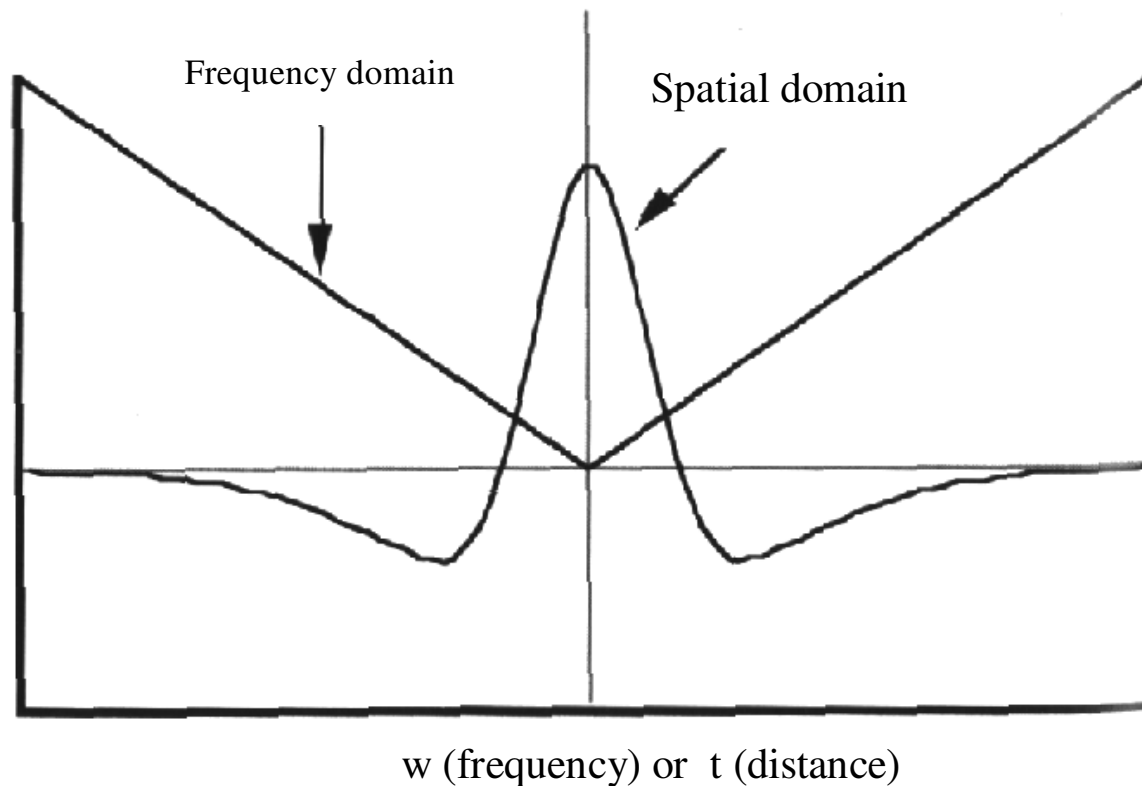
Backprojection of filtered data



The maximum spatial frequency is given by Nyquist's theorem by the distance T between two detector elements as

$$\omega_{\max} = 2\pi \cdot \frac{1}{2T}$$

The simple multiplication of $P_\theta(\omega)$ by ω in the frequency domain can be replaced by a convolution of $p_\theta(t)$ with the Fourier Transform of $|\omega|$ in the spatial domain:

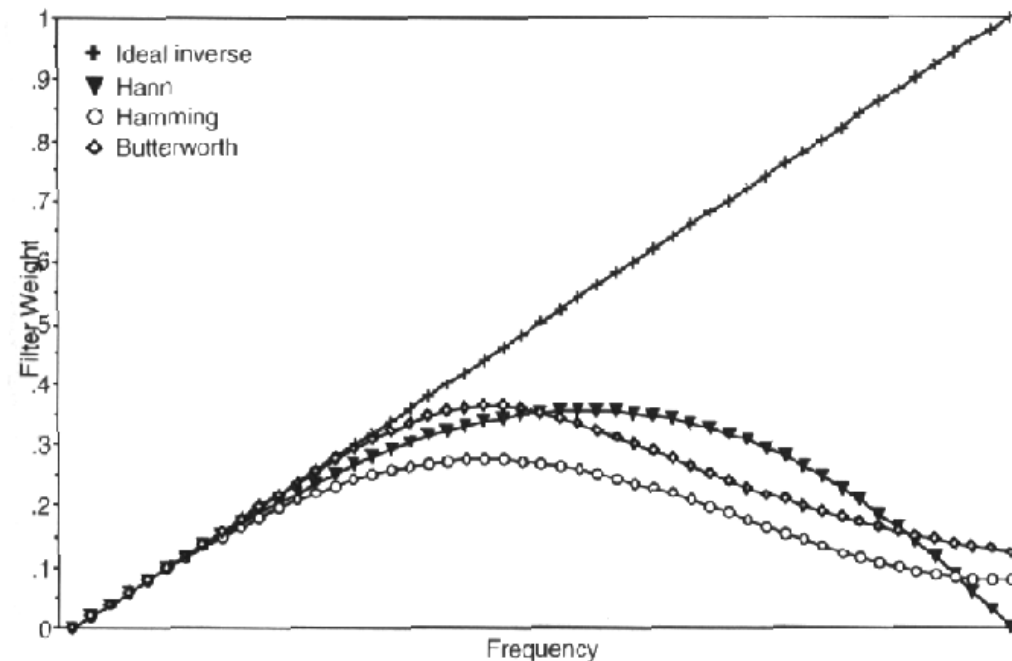


The ideal filter $|\omega|$ in spatial and frequency domain



Difficulties with the ideal filter $|\omega|$ occur with noisy data, as noise consists mainly of high frequencies, which are much enhanced by this filter.

Difficulties with the ideal filter $|\omega|$ occur with noisy data, as noise consists mainly of high frequencies, which are much enhanced by this filter. The ideal filter is therefore often replaced by special filter functions that decrease again towards high frequencies. For neutrons, the inherent beam unsharpness (see below) often attenuates most high frequencies towards the Nyquist limit.



The ideal filter $|\omega|$ and some alternative functions



2.4 **Number of projections**

The number of projections should be in the same order
as the number of rays in one projection.

2.4 Number of projections

The number of projections should be in the same order as the number of rays in one projection.

For M projections with N rays over 180° , the angular increment δ between two consecutive projections is given in fourier space as

$$\delta = \frac{\pi}{M}$$

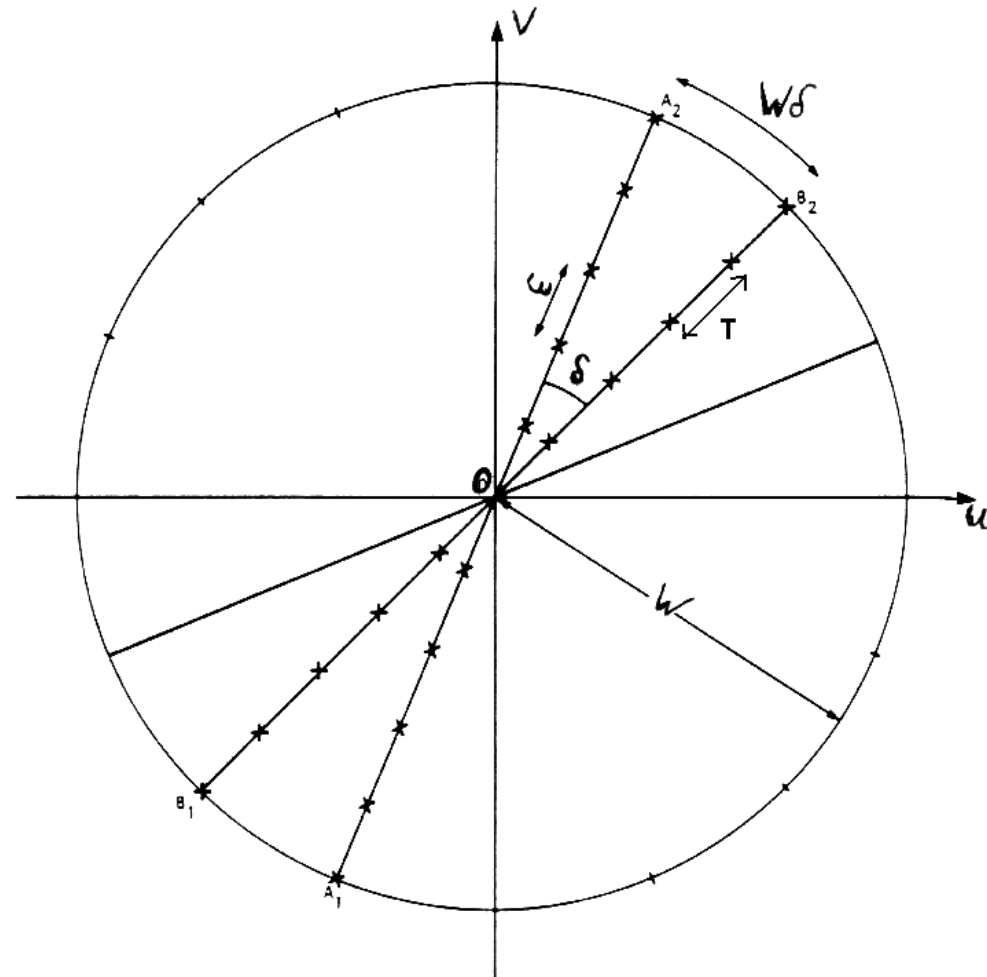
For distance T between two neighbouring rays, the highest measured spatial frequency ω_{\max} in the projection is given by Nyquist's Theorem as

$$\omega_{\max} = \frac{1}{2T}$$

This is the radius of a disk in the frequency domain that contains all measured values. The distance d between two consecutive values on the circle is

$$d = \omega_{\max} \cdot \delta = \frac{1}{2T} \frac{\pi}{M}$$

Density of measured values in frequency domain





For N measured values for each projection in spatial domain, there are also N measured values for each measured line in the frequency domain, so that the distance ε between two consecutive measured values on a radial line (or diameter) in frequency domain is given as

$$\varepsilon = \frac{2\omega_{\max}}{N} = \frac{1}{TN}$$



For N measured values for each projection in spatial domain, there are also N measured values for each measured line in the frequency domain, so that the distance ε between two consecutive measured values on a radial line (or diameter) in frequency domain is given as

$$\varepsilon = \frac{2\omega_{\max}}{N} = \frac{1}{TN}$$

For the worst azimuthal resolution in frequency domain to match the radial resolution, we must demand:

$$\frac{1}{2T} \frac{\pi}{M} \approx \frac{1}{TN}$$

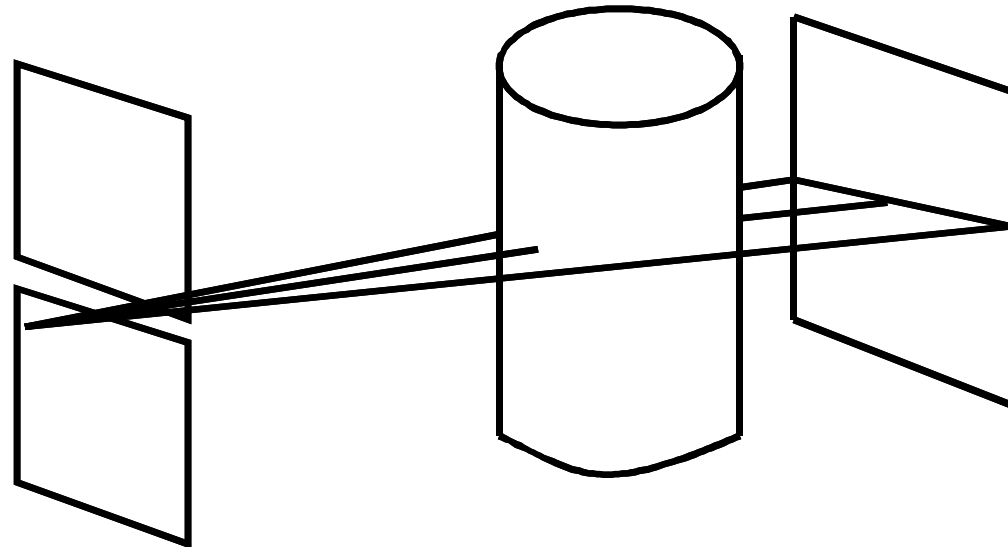
$$\frac{\textit{Number of projections}}{\textit{Number of rays}} = \frac{M}{N} \approx \frac{\pi}{2}$$

$$\frac{\textit{Number of projections}}{\textit{Number of rays}} = \frac{M}{N} \approx \frac{\pi}{2}$$

For practical neutron radiography, most detector systems cannot
- at least for sub-millimeter resolution - measure down to the
nominal Nyquist resolution given by their pixel size.

The greatest limiting factor is almost always the geometry of the
neutron beam and its deviation from the ideal parallel ray model.

Beam geometries for tomography



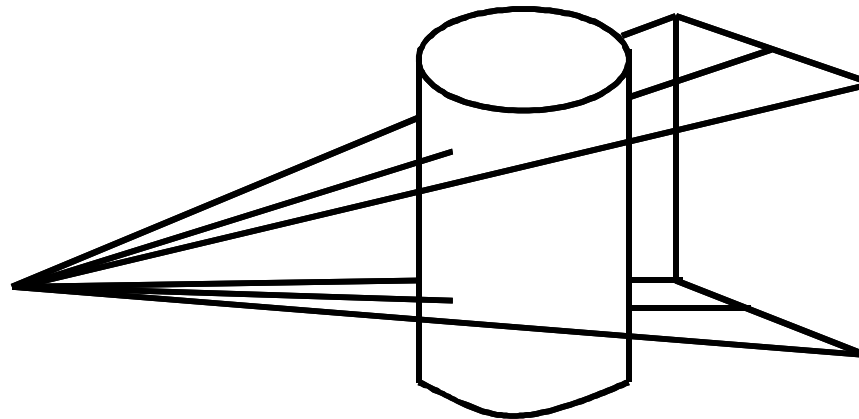
Fan beam geometry.

This applies for a standard setup with an X-ray tube and a line detector.

The projection of the sample is magnified.

Reconstruction is done in an even plane.

Beam geometries for tomography

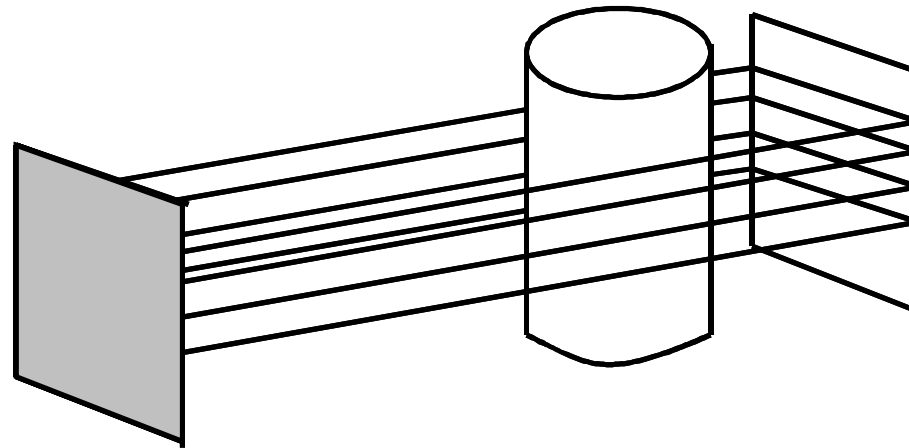


Cone beam geometry.

Applies for a point source (LinAc, X-ray tube) and a two-dimensional detector.

The projection of the sample is magnified.
Reconstruction must be done in a 3D-Matrix.

Beam geometries for tomography



Parallel beam geometry.

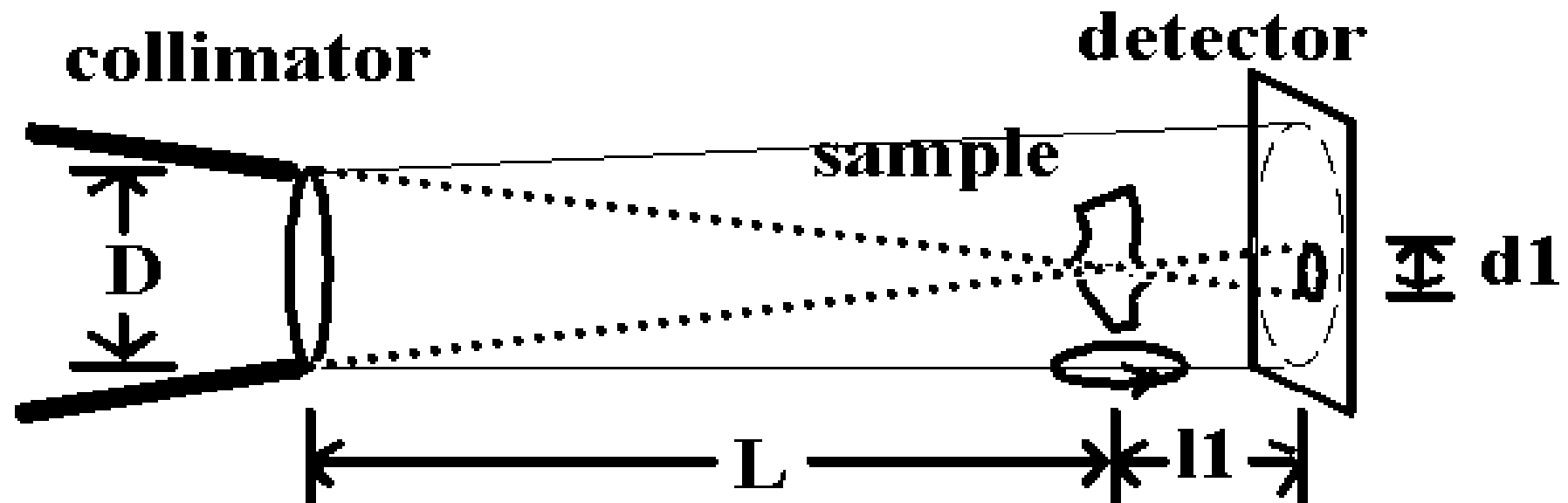
The simplest case - applies for a synchrotron light source and a linear 2D-detector.

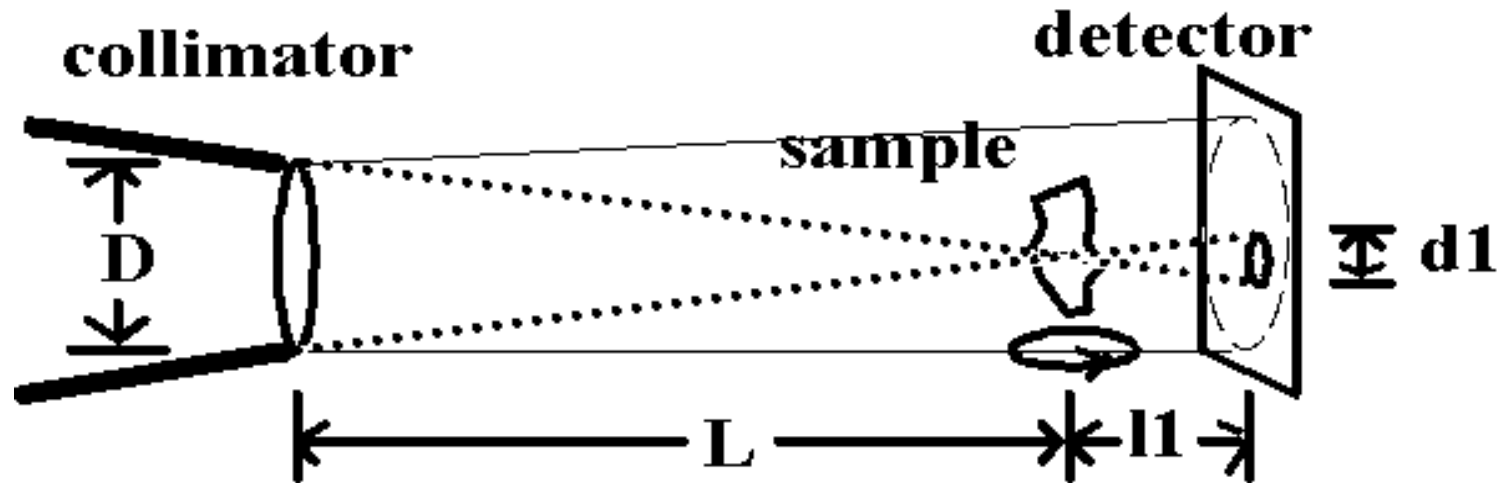
There is no magnification.

For neutrons, none of the cases is really true,
we try to approximate parallel beam geometry as good as possible.

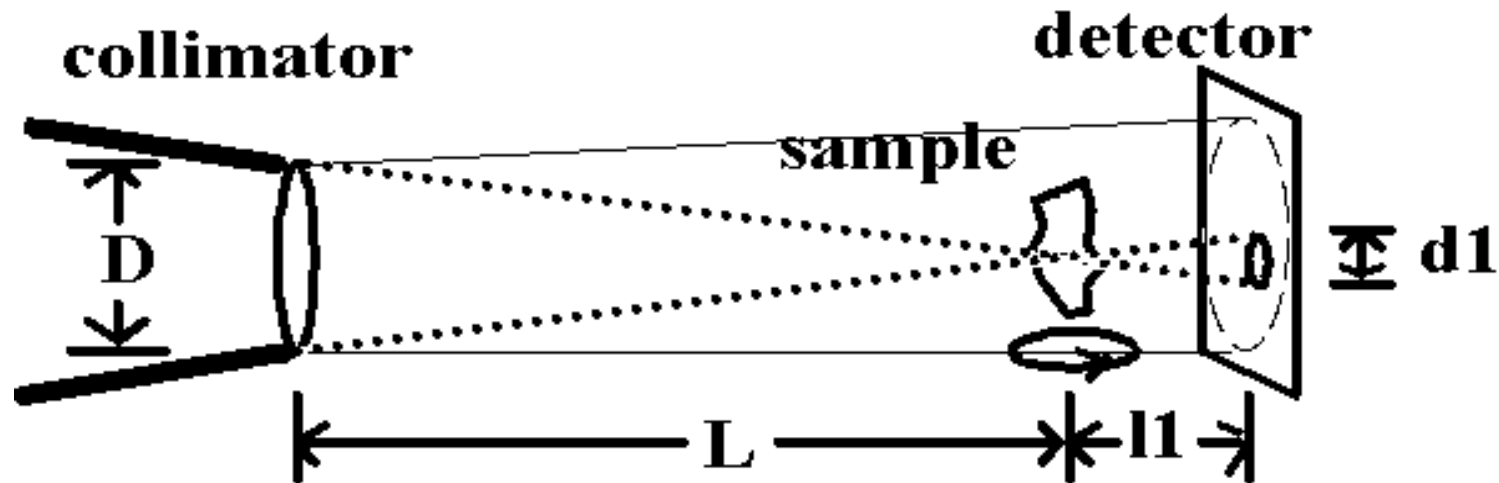
The neutron case - flight tube vs. beam guide

For all cases, the angle of the source seen from the sample position determines the achievable resolution of a projection, assuming an ideal detector of infinite resolution.



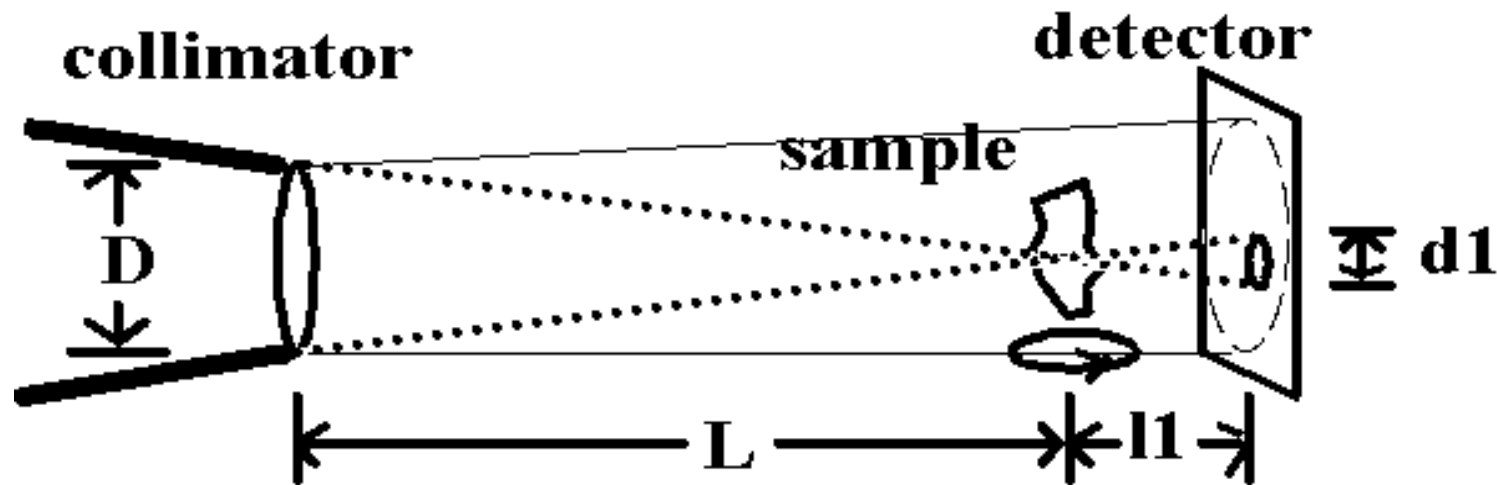


The parameter to characterize a radiography setup is the inverse tangential of the opening angle, given as the ratio L/D of the source-to-sample-distance L vs. the source diameter D .



The parameter to characterize a radiography setup is the inverse tangential of the opening angle, given as the ratio L/D of the source-to-sample-distance L vs. the source diameter D .

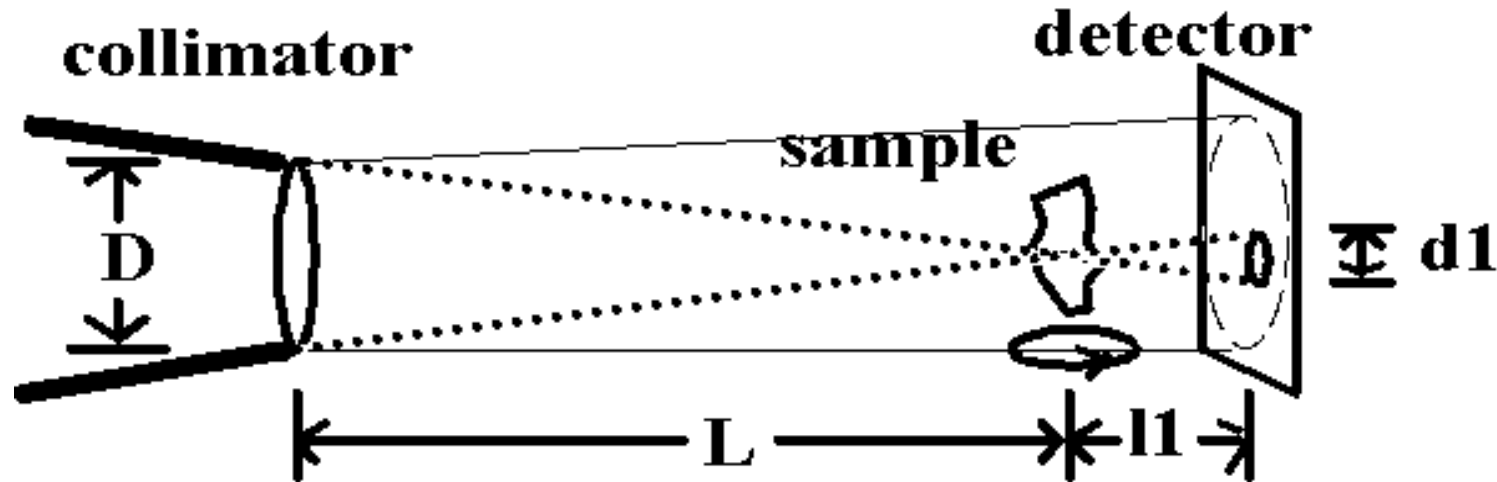
For a classical radiography setup, D is the diameter of a diaphragm in the beam path.



The parameter to characterize a radiography setup is the inverse tangential of the opening angle, given as the ratio L/D of the source-to-sample-distance L vs. the source diameter D .

For a classical radiography setup, D is the diameter of a diaphragm in the beam path.

An infinitesimal volume element of the sample is projected onto a circle on the detector.



The parameter to characterize a radiography setup is the inverse tangential of the opening angle, given as the ratio L/D of the source-to-sample-distance L vs. the source diameter D .

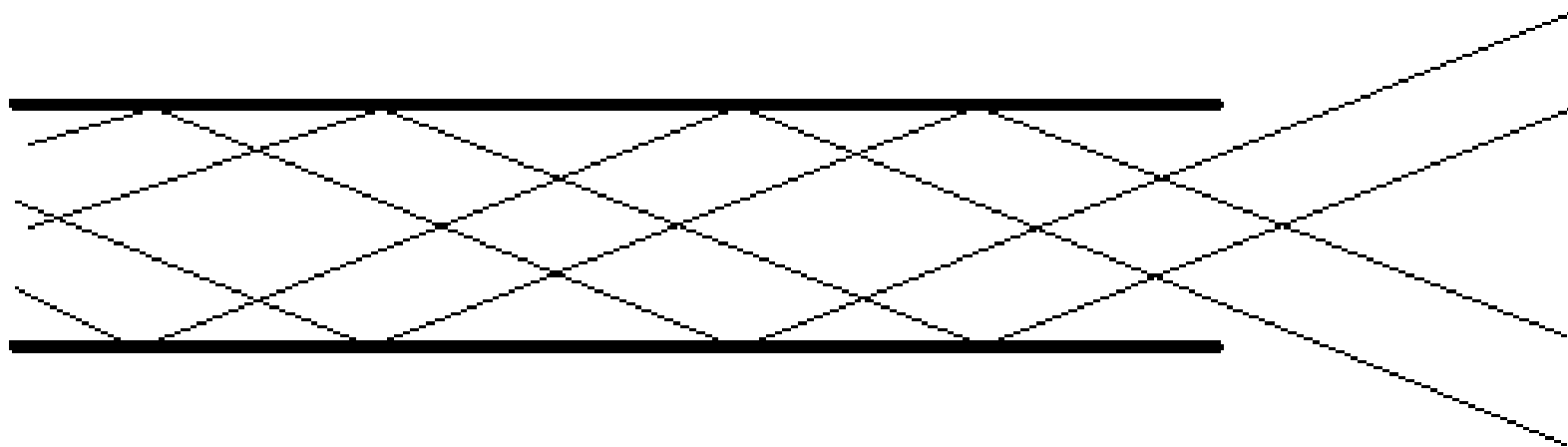
For a classical radiography setup, D is the diameter of a diaphragm in the beam path.

An infinitesimal volume element of the sample is projected onto a circle on the detector.

This image blur can be expressed as $d1=l1/(L/D)$, the magnification can be expressed as $M=L/(L-l1)$.

If radiography is performed at the end of a neutron guide, the divergence of the beam is given by the critical angle of reflection γ_c of the neutron guide.

The divergence is constant within the cross section of a straight neutron guide, it acts like a divergent area source.



Beam geometry at a neutron guide



Slow neutrons can be totally reflected from surfaces up to a critical angle of

$$\gamma_c = \sqrt{2(1-n)} = \lambda \sqrt{\frac{Na}{\pi}} \approx 10^{-3} \dots 10^{-2}$$

N is the atomic density of the wall material, a the coherent scattering length, and λ the neutron wavelength .

Slow neutrons can be totally reflected from surfaces up to a critical angle of

$$\gamma_c = \sqrt{2(1-n)} = \lambda \sqrt{\frac{Na}{\pi}} \approx 10^{-3} \dots 10^{-2}$$

N is the atomic density of the wall material, a the coherent scattering length, and λ the neutron wavelength .

For a guide coated with natural nickel, we get
 $\gamma_c = 1.73 \cdot 10^{-3} \text{ rad / \AA}$, or $0.1^\circ / \text{\AA}$.



The beam divergence becomes dependent on the wavelength,
and we need to calculate an "effective" L/D -ratio which determines
the quality of a projection.



The beam divergence becomes dependent on the wavelength, and we need to calculate an "effective" L/D -ratio which determines the quality of a projection.

If the spectrum is known, we can roughly estimate L/D by calculating the arithmetic mean value of all wavelengths as λ_{av} and by substituting λ_{av} , we can calculate

$$L/D = 1/\tan(2\gamma_c).$$



The beam divergence becomes dependent on the wavelength, and we need to calculate an "effective" L/D -ratio which determines the quality of a projection.

If the spectrum is known, we can estimate L/D by calculating the arithmetic mean value of all wavelengths as λ_{av} and by substituting λ_{av} , we can calculate

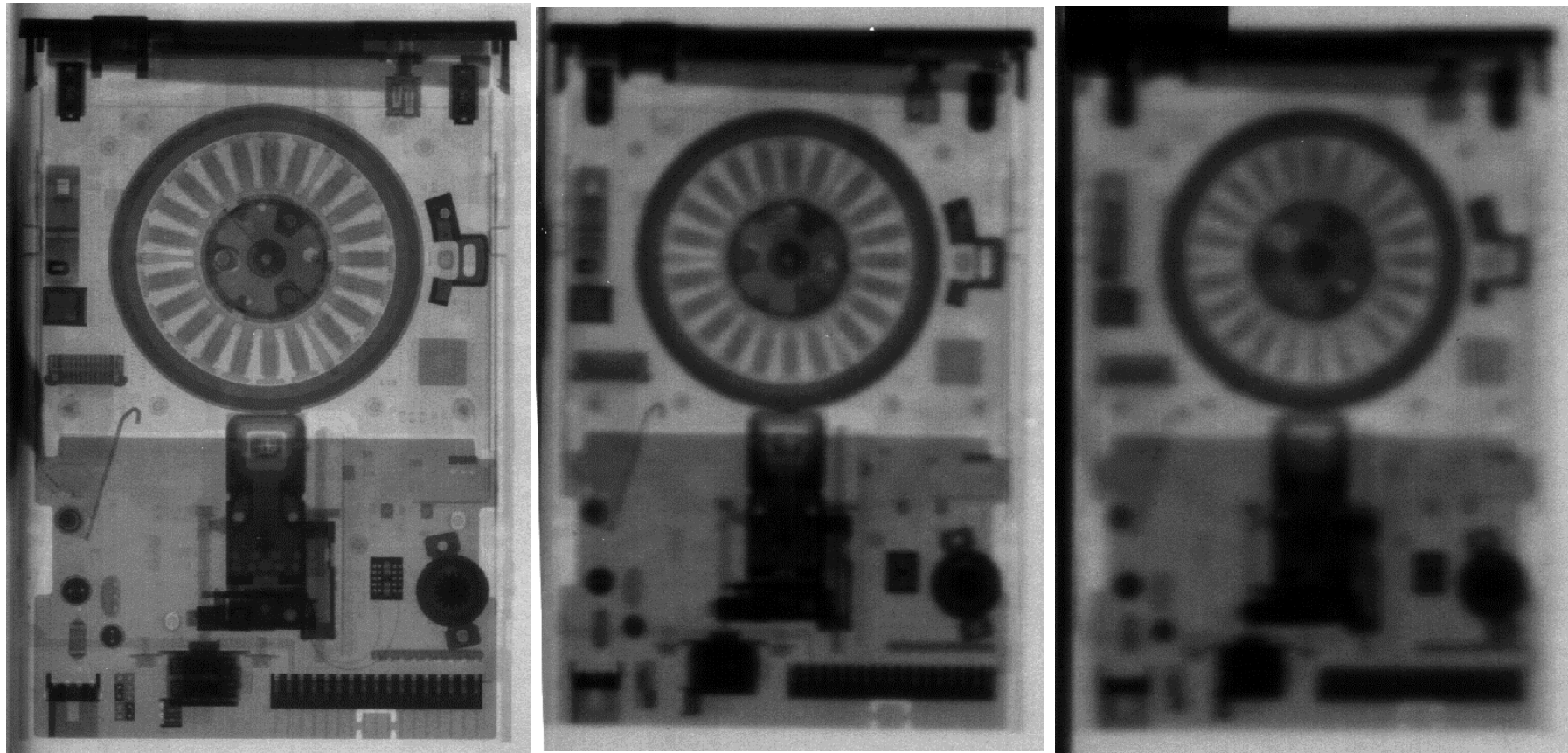
$$L/D = 1/\tan(2\gamma_c).$$

Still, a more accurate calculation has to take into account the angular distribution for each wavelength, integrated over all wavelengths.

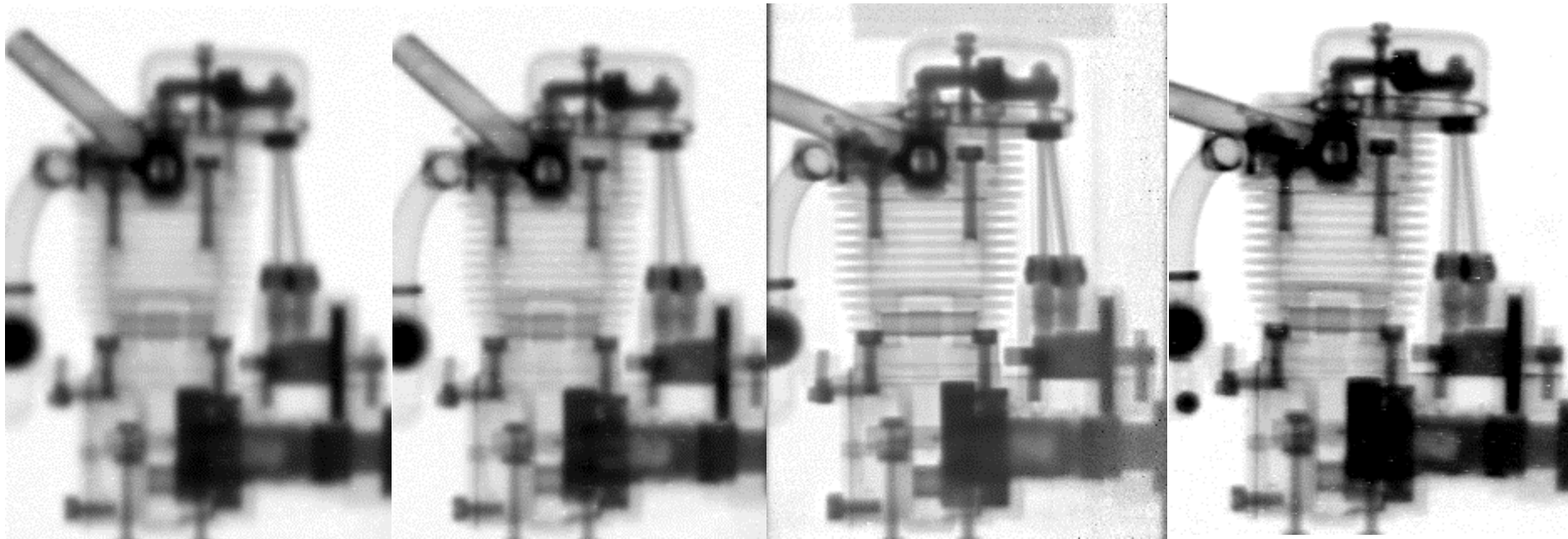


A Neutron guide is not a good choice for a neutron radiography facility,
as can be shown by the measurements below.

A Neutron guide is not a good choice for a neutron radiography facility,
as can be shown by the measurements below.



Radiographs of a 3,5" floppy drive in 0 cm , 10 cm and 20 cm distance
from a film + Gd sandwich taken at a cold neutron guide with $L/D=71$.



$L/D=71$

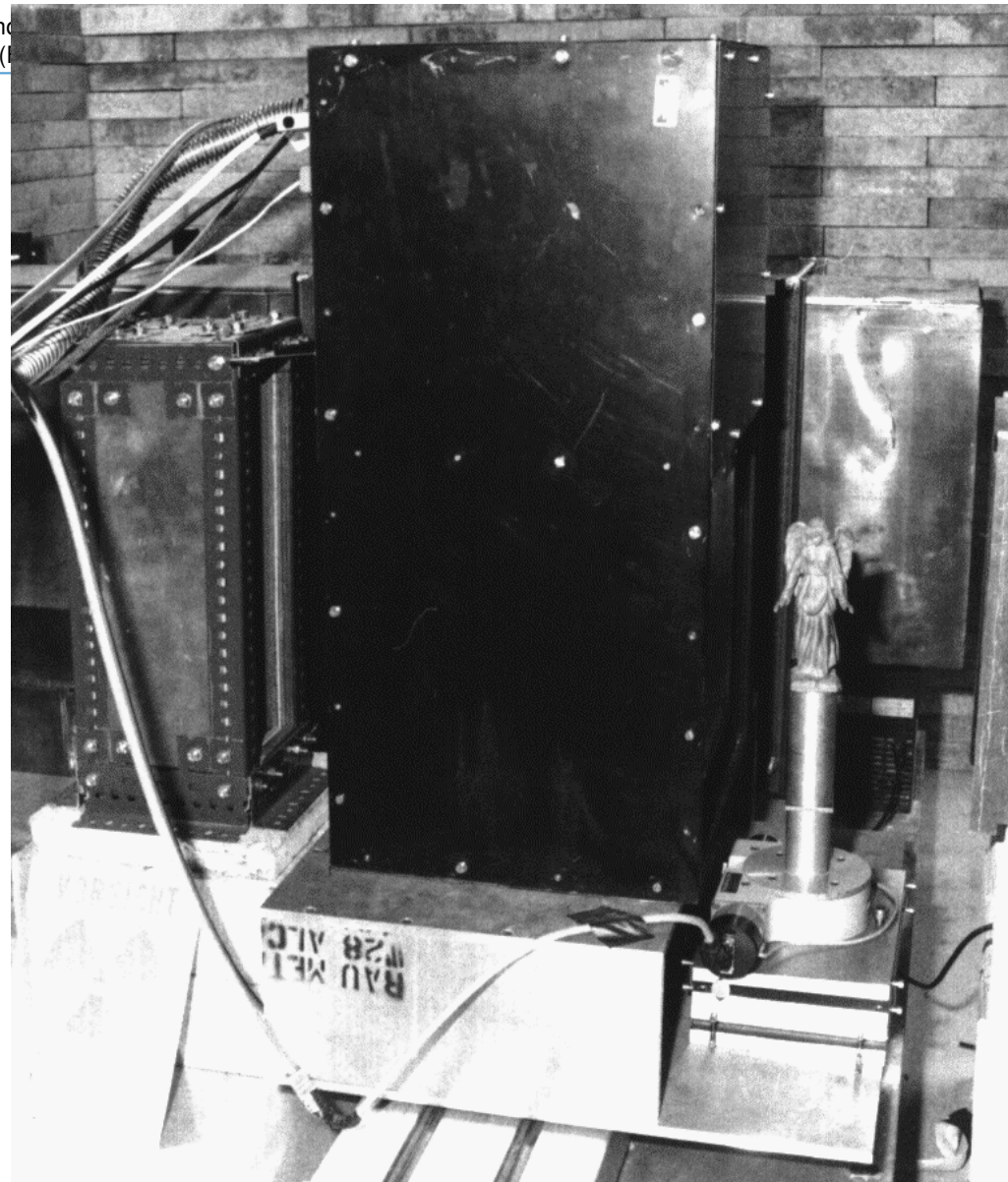
$L/D=115$

$L/D=320$

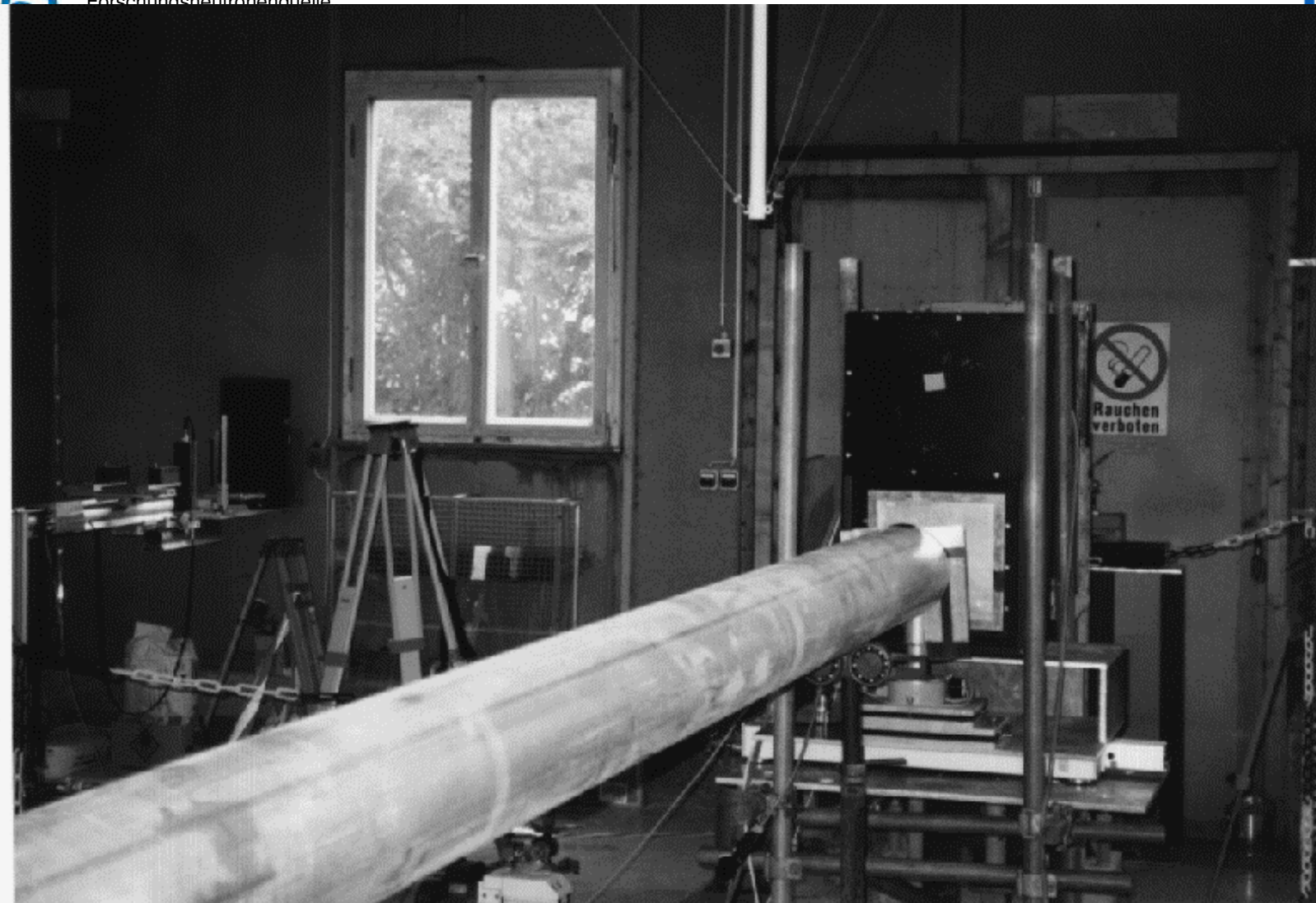
$L/D>500$.

Radiographs of a small motor taken at different beam positions
with different L/D ratios.

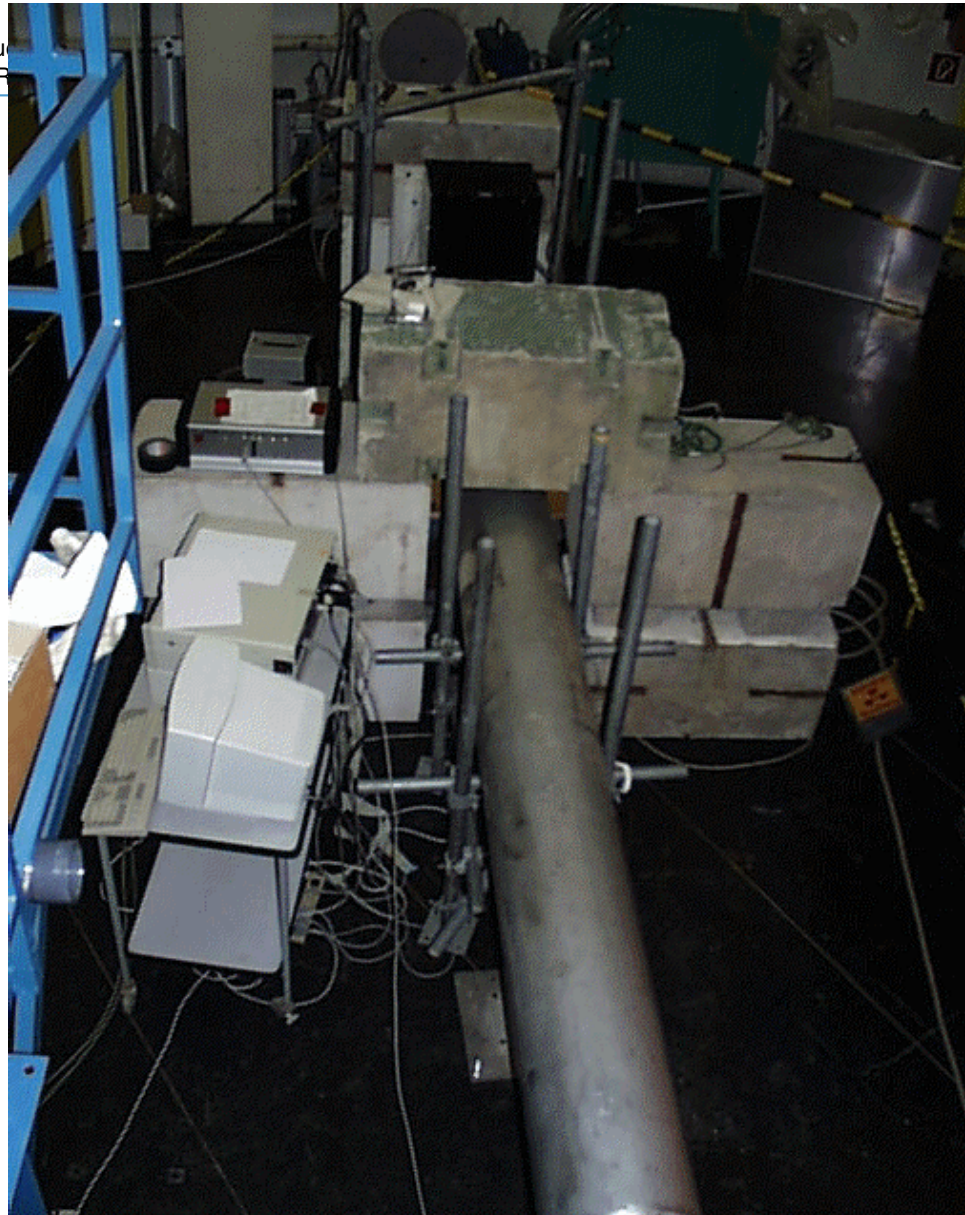
The radiographs were taken at a cold guide, a thermal guide,
a cold guide with a consecutive 15 mm pinhole and 4.8 m flight tube
and at a classical 20 mm pinhole and 10 m flight tube arrangement.



Tomography setup at a neutron guide

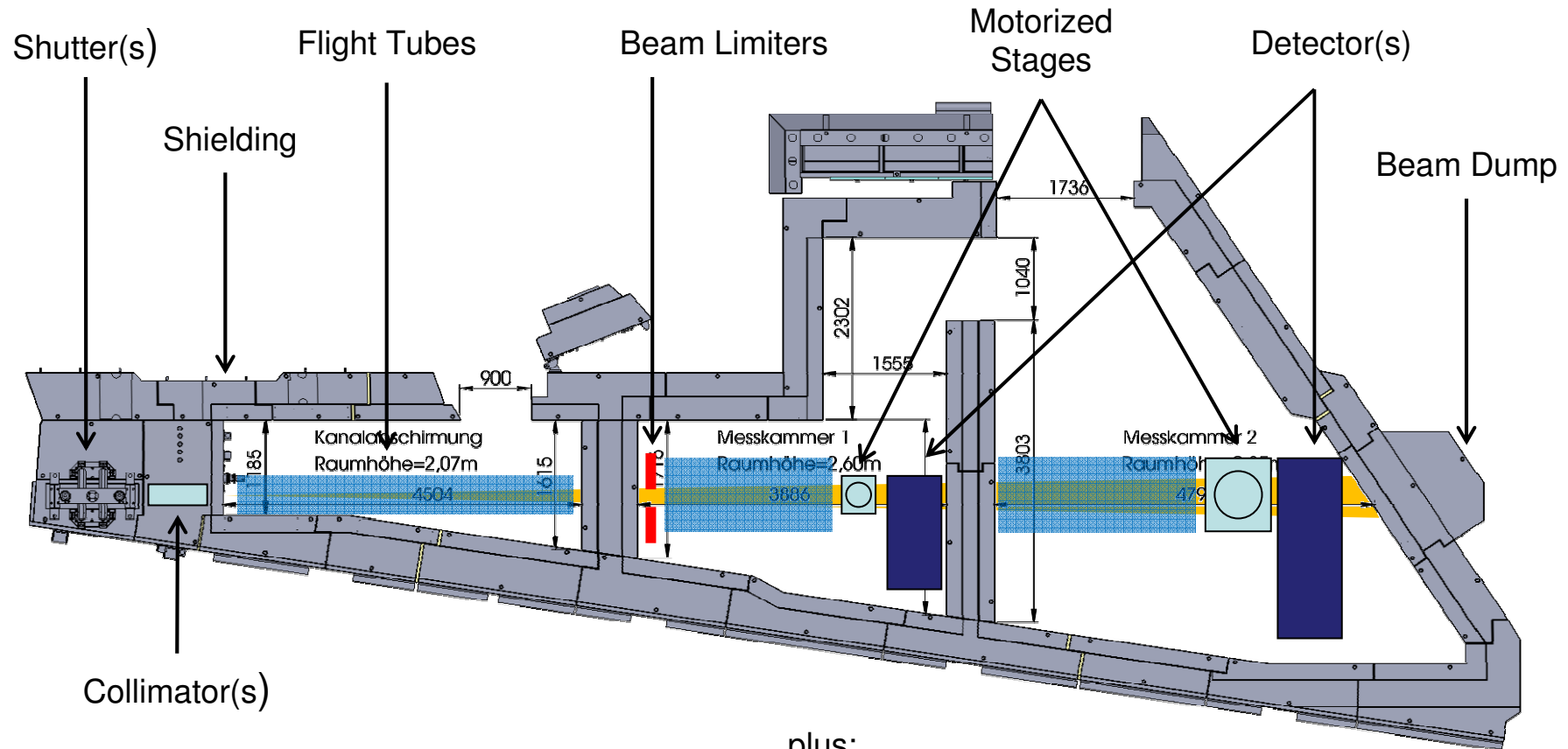


Combination of neutron guide and flight tube



Dedicated radial flight tube at old FRM Munich - shielding incomplete

ANTARES NI beamline



optional:
-Beam Filters
-Monochromator / Selector

plus:
-Access Control
-Media Supply (electricity, gas, water, ...)
-IT (network, storage, servers, software, ...)